Negative group velocity of surface plasmons on thin metallic films

Yongmin Liu, David F. P. Pile, Zhaowei Liu, Dongmin Wu, Cheng Sun, Xiang Zhang*

NSF Nanoscale Science and Engineering Center (NSEC), 5130 Etcheverry Hall,
University of California, Berkeley, California 94720-1740

ABSTRACT

By tailoring the dispersion curve of surface plasmons (SPs) of a thin metallic film surrounded by dielectric half-spaces, it is shown that the group velocity of the symmetric mode is always positive, while the group velocity of the anti-symmetric mode can be negative. Consequently, the forward and backward propagation of SPs, in which the energy flow is respectively parallel or antiparallel to the wave vector, can be realized. The physical origin of the intriguing backward SPs is given. Furthermore, schemes for the negative refraction and imaging of SPs are proposed by incorporating two plasmon modes with group velocities of opposite signs.

Keywords: thin film, surface plasmon, negative group velocity, negative refraction

1. INTRODUCTION

Recently, there has been explosive interest in negative index materials (NIMs), which were proposed by Veselago almost forty years ago.[1] Many counterintuitive phenomena associated with NIMs, such as the reversed Snell's law and reversed Cerenkov radiation have been demonstrated.[2, 3] Moreover, NIMs can form perfect lenses beating the diffraction limit, the barrier for sub-wavelength imaging resolution in conventional optics.[4] So far, metamaterials and photonic crystals (PCs) are the two major approaches to realize NIMs.[5, 6] Based on artificial split ring resonators and metallic wires to engineer the effective permeability (μ_{eff}) and permittivity (ε_{eff}), respectively, metamaterials are able to achieve negative refractive index (n_{eff}) when μ_{eff} and ε_{eff} are simultaneously negative.[7] On the other hand, photonic crystals can behave as materials having negative n_{eff} controllable by the band structure.[8] Both metamaterials and photonic crystals have shown negative refraction at microwave frequencies, but fabrication of nano-structures suitable for similar experiments at visible wavelengths is challenging. For nearly isotropic media, the key ingredient for negative refraction is that the group velocity opposite to the phase velocity.[7, 8]

In this paper, we intend to propose a scheme to extend the novel phenomenon of negative refraction to surface plasmons (SPs) on thin films. SPs are collective electron oscillations that are coupled to electromagnetic waves at the interface between dielectrics and metals.[9] Since SPs are highly confined at the interface and are very sensitive to surrounding media, they are widely used in bio-sensoring and surface enhanced Raman scattering (SERS). Moreover, since the wavelength of SPs can be much smaller than that of electromagnetic waves at the same frequency there are promising applications of SPs in sub-wavelength lithography, optical devices and imaging.[10, 11] Sub-diffraction-limited images with 60nm half-pitch resolution (one-sixth of the illumination wavelength) have been successfully achieved.[12]

To explore the feasibility of negative refraction of SPs, in this paper, we study the group velocity of SPs on a thin metallic film surrounded by dielectrics. It is shown that the group velocity of the anti-symmetric plasmonic mode can be negative by engineering the dispersion curve. Numerically, we demonstrate intriguing backward propagation of SPs in which direction of the group velocity is opposite to the wave vector, in contrast to forward SPs with the group velocity and wave vector in the same direction. Finally, a structure to demonstrate the negative refraction and imaging of SPs is proposed. Our results indicate a new way to control the propagation of SPs, which are important for nano-scale manipulation of optical waves.

---

* Correspondence author. Email: xiang@berkeley.edu

2. THEORECTIAL BACKGROUND

Surface plasmons (SPs) are surface electromagnetic excitations that can propagate in a wave-like fashion along the interface between a dielectric and a metal medium. The dielectric function of metals can be well described by Drude model:

$$\varepsilon_m(\omega) = \varepsilon_\infty - \frac{\omega_p^2}{\omega(\omega - i\gamma)} \tag{1}$$

where ε_∞ is the permittivity of the metal at infinite frequency, ω_p is the bulk plasma frequency depending on the electron density and mass, and γ is the damping term resulting from electron-phonon and electron-electron collisions. At the interface of a semi-infinite metal and a dielectric material with permittivity ε_d, SPs exist within the frequency range from $\omega = 0$ up to $\omega = \omega_p / \sqrt{\varepsilon_\infty + \varepsilon_d}$. Suppose the z-axis is normal to the interface and that SPs propagate along the x-axis as shown in Fig. 1(a), then the dispersion relation for SPs at the interface between a semi-infinite metal and a dielectric half-space satisfies

$$\varepsilon_m(\omega) k_z^d + \varepsilon_d k_z^m = 0 \tag{2}$$

where the z-component of the wave vector in the dielectric and metal are given by

$$k_z^d = \sqrt{k_x^2 - \varepsilon_d \frac{\omega^2}{c^2}} \tag{3}$$

and

$$k_z^m = \sqrt{k_x^2 - \varepsilon_m(\omega) \frac{\omega^2}{c^2}} \tag{4}$$

respectively. Note k_x is continuous because of the conservation of tangential momentum at the interface.

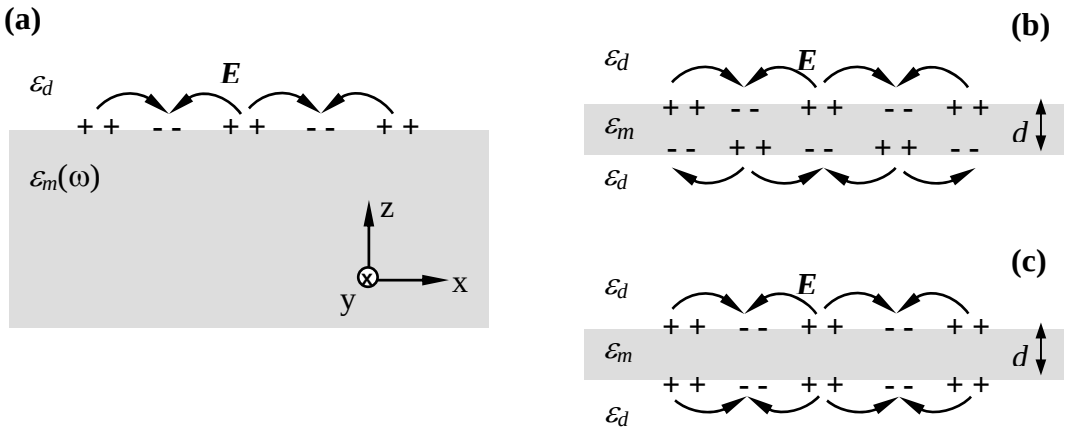

Fig. 1. The schematic illustration of the charge density fluctuation and electric field of different surface plasmon modes. (a) Surface plasmon mode at the interface between a semi-infinite dielectric and metal; (b) Antisymmetric plasmon mode of a thin metal film with thickness *d*; (c) Symmetric plasmon mode of a thin metal film with thickness *d*.

When a metallic film is embedded in dielectric media and the film thickness *d* is smaller than the penetration depth of SPs, the interaction between the two SPs on the two metal-dielectric interfaces cannot be neglected.[9, 13-15] The coupled modes are generally called antisymmetric and symmetric plasmon modes. Here, we define the antisymmetric and

symmetric modes with respect to the charge distribution across the two interfaces, as schematically shown in Fig. 1(b) and Fig. 1(c), respectively. The dispersion relations for the anti-symmetric and symmetric modes follow as:

$$\omega^{+}: \ \varepsilon_m(\omega)k_z^d + \varepsilon_d k_z^m \tanh(\frac{k_z^m d}{2}) = 0 \tag{5}$$

$$\omega-: \ \varepsilon_m(\omega)k_z^d + \varepsilon_d k_z^m \coth(\frac{k_z^m d}{2}) = 0 \tag{6}$$

respectively. Obviously, when the film is thick, Eqs. (5)-(6) reduce to the dispersion curve for SPs at a semi-infinite metal-dielectric interface (see Eq. 2).

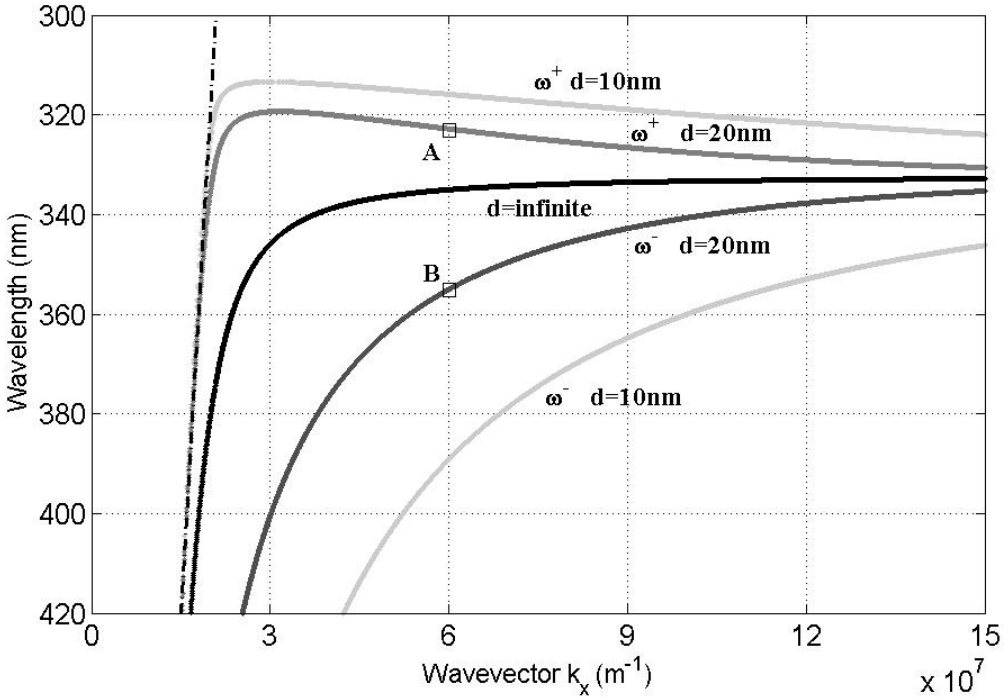

Fig. 2. Dispersion curve of surface plasmons for semi-infinite silver-air interface ($d \to \infty$), as well as for a thin silver film (*d=20, 10nm*) surrounded by air. The dash-dot line represents the light line in vacuum. When the film thickness reduces, two surface plasmon modes, *i. e.*, antisymmetric (ω^+) and symmetric modes (ω^-) exist. The antisymmetric mode can possess a negative slope, implying the group velocity ($v_g = d\omega/dk$) is negative. Point A ($k_x = 6\times10^7\, m^{-1}, \omega = 2\pi c/\lambda = 5.84\times10^{15}\, rad/s$) in the antisymmetric band, and point B ($k_x = 6\times10^7\, m^{-1}, \omega = 2\pi c/\lambda = 5.31\times10^{15}\, rad/s$) in the symmetric band are chosen for demonstrating the forward and backward propagating surface waves, respectively (see the text).

Figure 2 represents the dispersion relation of SPs at the interface between semi-infinite silver and air, as well as for a thin silver film (d =10 and 20 nm) surrounded by air. The Drude model for silver is taken as $\varepsilon_{silver}(\omega) = 6 - \frac{(1.5\times10^{16})^2}{\omega(\omega - 7.73\times10^{12}i)}$,[16] where the damping term is purposely chosen as 10% of the real value in order to increase the SP propagation length for clear demonstration in the following numerical simulations. From Fig. 2, it can be seen that all the dispersion curves lie on the right of the light line, which means SPs have a larger wave vector than electromagnetic waves of the same frequency (if this were not that case, then the SPs would be radiating into the surrounding dielectric, *i.e.* the SPs would not exist). As wave vector k is sufficiently large, the frequency approaches the

cut-off given by $\omega_{sp} = \omega_p / \sqrt{\varepsilon_\infty + \varepsilon_d} = 5.67 \times 10^{15} rad/s$. Interestingly, if d is sufficiently small, the antisymmetric mode (the higher-frequency SP band) possesses negative slope at the large wave vector region, indicating the group velocity ($v_g = d\omega / dk$) is negative. For example, in the dispersion curve for a 20nm-thick silver, after the threshold of $k_x \approx 3.25 \times 10^7 m^{-1}$, the dispersion curve of the antisymmetric mode tends downward until the cut-off frequency. In contrast, the slope of the SP dispersion curve for the symmetric mode is always positive.

When k_x is sufficiently large, both the antisymmetric and symmetric modes approach the cut-off frequency $\omega_{sp} = \omega_p / \sqrt{\varepsilon_\infty + \varepsilon_d} = 5.67 \times 10^{15} rad/s$ for SPs at a semi-infinite interface between silver and air. Physically this is because for large k_x, the penetration depth of SPs into the metal is small compared with the film thickness, and therefore SPs at each interface (for both antisymmetric and symmetric modes) are decoupled.

3. RESULTS AND DISSCUSION

3.1 Backward and forward surface plasmons

Now we consider different propagation characteristics of SPs with opposite group velocities. FEMLAB, a commercial electromagnetic eigenmode solver based on the finite element algorithm is used in the numerical simulation (the results have been confirmed using an our own finite difference algorithm). The simulation domain consists of a 200nm high-index slab as a prism, a 50nm air gap, a 20nm silver film and a 130nm air layer with open boundary conditions applied at the edges of the computational window. A Gaussian beam with a finite waist and TM polarization (magnetic field is along y axis) is incident from the high-index prism and the incident angle is 45°. The incident light is not only reflected from the prism-air interface, it can also resonantly excite the SP mode through the evanescent wave penetrating from the prism into the air gap (due to the total internal refraction) if the tangential component of the wave vector is matched to that of the desired SP mode.

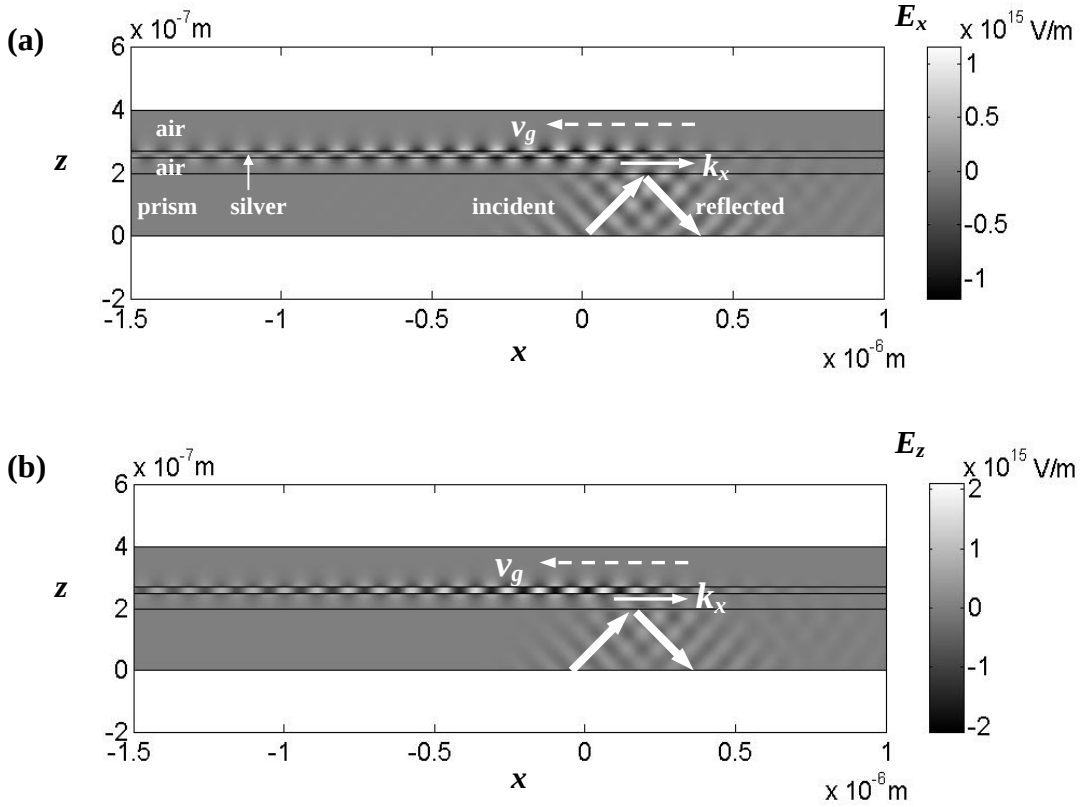

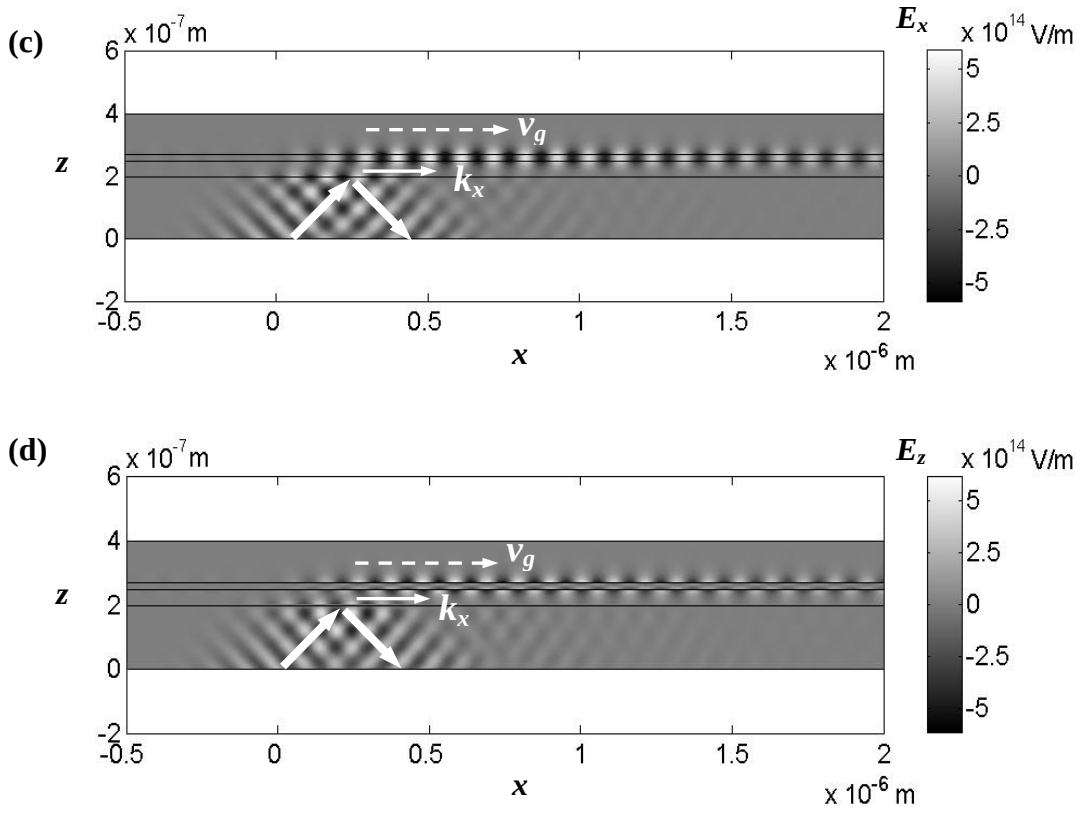

Fig. 3. Field profile of backward and forward propagating surface plasmons. (a) E_x component and (b) E_z component of electric fields when an antisymmetric mode (point A in the dispersion curve of a 20nm silver film in Fig. 2, where $k_x = 6\times10^7 m^{-1}, \omega = 2\pi c/\lambda = 5.84\times10^{15} rad/s$) is excited by total internal reflection. The surface wave propagates leftwards that is opposite to the wave vector k_x, indicating the group velocity $v_g = d\omega/dk$ is negative in the x-direction. (c) E_x component and (b) E_z component of electric fields when a symmetric mode (point B as marked in Fig. 2, where $k_x = 6\times10^7 m^{-1}, \omega = 2\pi c/\lambda = 5.31\times10^{15} rad/s$) is resonantly excited. The surface wave propagates forward, *i.e.*, parallel to wave vector k_x, indicating the group velocity $v_g = d\omega/dk$ is positive.

When the refractive index of the prism equals 4.36, the SP mode with $k_x = 6\times10^7 m^{-1}$ and $\omega = 2\pi c/\lambda = 5.84\times10^{15} rad/s$ (point A marked in Fig. 2) can be excited. The *x*-component of the electric field as shown in Fig. 3 (a) has larger magnitude at the silver-air interface, which is due to the enhancement related to resonant excition of the SPs by the attenuated total reflection. More importantly, it can be seen that the surface wave propagates leftwards and gradually decays. It should be noted that the tangential component of the momentum is always continuous across the interfaces, *i.e.*, k_x always points to the right (following from the angle of the incident wave). Therefore, the field profile in Fig. 3(a) indicates that the group velocity is antiparallel to the phase velocity, which is predicted by the negative slope of the dispersion curve in Fig. 2. The E_z component is shown in Fig. 3(b) and again we can see that the surface wave propagates backward, compared with the positive phase velocity in the x-direction. Figs. 3(a) and 3(b) also confirms that the charge density fluctuation for the antisymmetric mode is opposite at the top and bottom silver-air interfaces, which is schematically shown in Fig. 1 (b), *e.g.* the *x*-component of the field is antisymmetric (across the film) which must be related to antisymmetric distribution of the charges.

The symmetric SP mode marked as point B in Fig. 2 ($k_x = 6\times10^7 m^{-1}$ and $\omega = 2\pi c/\lambda = 5.31\times10^{15} rad/s$) is excited when the prism has n = 4.79. In contrast to what one can see in Figs. 3(a) and 3(b), the field profile in Figs. 3(c) and 3(d) indicates the surface plasmon propagates forwards; that is, both the group velocity and phase velocity are positive in the

x-direction. Moreover, the charge density distribution is symmetric with respect to the central line of the silver film (notice the symmetric distribution of the *x*-component of the electric field across the film).

3.2 Physical origin of backward and forward surface plasmons

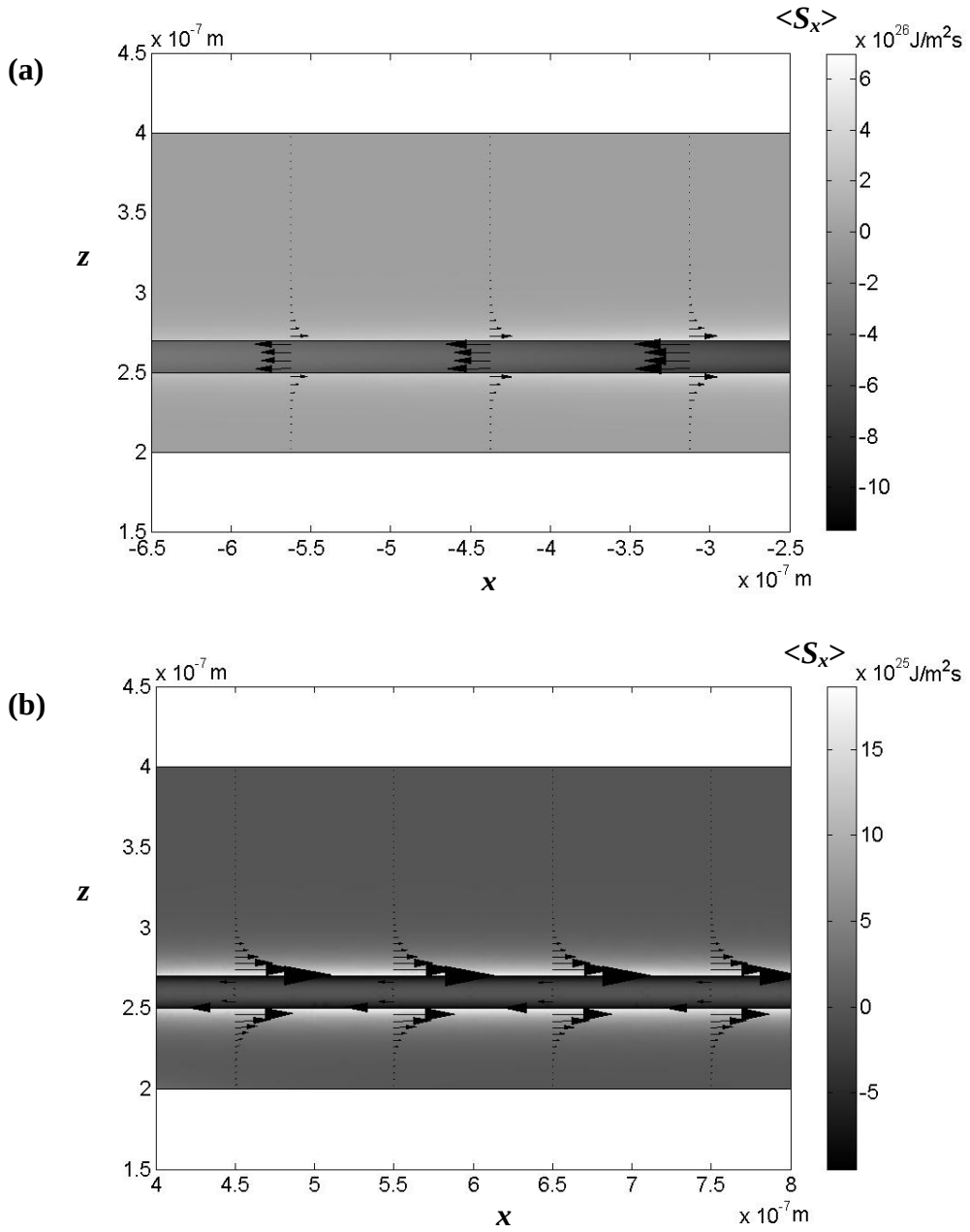

Fig. 3. Time-averaged *x*-component of Poynting vector ($<S_x>$) for different surface plasmon modes. (a) The SP mode as marked as A in Fig. 2, whose group velocity is negative. (b) The SP mode as marked as B in Fig. 2, whose group velocity is positive. In both (a) and (b), $<S_x>$ is negative inside the metal, but positive in the surrounding air layer. Overall, more power flows in the metal (compared to in the dielectric regions) for a SP mode with a negative group velocity; while more power flows in the dielectric for a SP mode with a positive group velocity.

The physical origin of the backward and forward surface plasmons can be explained by considering the *x*-component of Poynting vector (S_x), which represents the power-flow parallel to the surface. From the Maxwell's equations, it is straightforward to derive the time-averaged S_x , which satisfies [17]

$$< S_x >= \frac{1}{2}\mathrm{Re}(E_z H_y^*) = \frac{1}{2}\mathrm{Re}((\frac{\partial}{\partial x} H_y) H_y^*) \propto \frac{k_x}{\varepsilon} \tag{7}$$

For metal, $\varepsilon_m(\omega)$ is negative for the whole frequency region when surface plasmons exist. Equation (7) suggests that $<S_x>$ is always negative inside the metal and always positive in the dielectric. Therefore the power flow is opposite to the phase velocity (represented by k_x) in the metal. In contrast, $< S_x >$ is parallel to the phase velocity in normal dielectric materials, because of positive ε_d . Note the group velocity has the same direction as the net power flow (integral of S_x over all *z*).

Depending on the thickness of metal film, the working frequency and wave vector k_x , the net power-flow of the mode (considering both the metal film and surrounding media) can be negative. In other words, a higher proportion of power should flow through the metal than the dielectric to achieve negative group velocities of SPs. Figure 3(a) and (b) represent the time-averaged S_x for point A and B marked in Fig. 1, respectively. It can be seen that inside the metal, $<S_x>$ is negative for both cases, while $<S_x>$ is positive for the surrounding dielectric media. However, the integral of $<S_x>$ over *z* along a line normal to the film interfaces shows that the net power-flow is indeed negative for SPs with negative group velocity as shown in Fig. 3(a), while positive for SPs with positive group velocity as shown in Fig. 3(b).

3.3 Negative refraction and imaging of surface plasmons

We have confirmed the existence of negative group velocity of SPs on thin films, and explained the physical reason. An interesting question arising is what happens at the interface between two regions supporting forward and backward SPs respectively. Recalling the case of an electromagnetic wave propagating toward the interface between a positive-index material and a negative-index material,[7, 8] we can expect that negative refraction of SPs emerges, because the conservation of the tangential component of momentum and Causality theorem have to be satisfied at the boundary as schematically illustrated in Fig. 4. Very recently, the sub-wavelength imaging of SPs has been reported based on the negative refraction of surface modes at the interface between a semi-infinite metal (with dielectric halfspace) and a structure consisting of a narrow dielectric gap between metal halfspaces.[18]

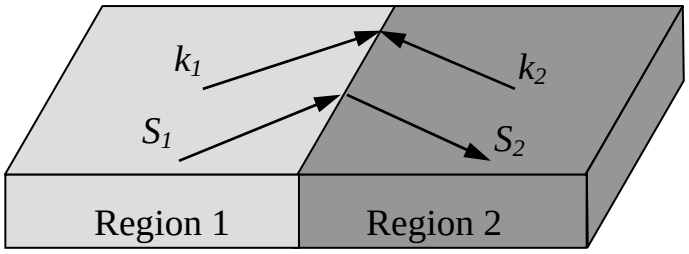

Fig. 4. Schematic illustration for negative refraction of surface plasmons. Region 1 supports a SP mode with a positive group velocity, and region 2 supports a SP mode with a negative group velocity.

One important issue for demonstrating the negative refraction or imaging of SPs is the mode matching. In other words, we should carefully select the two SP modes in order to avoid large reflections and scatterings at the boundary. Quantitively, we need to consider three factors to increase the coupling efficient of SPs from one region to the other one. First is the field profile, which gives rise to strong scattering if it is not matched; Second is the SP penetration depth,

which also contribute to the scattering; The last one is effective phase-index determined by k_x, which leads to reflection. It should be noted that the mode matching is a rather complicated process, and we will discuss it in detail elsewhere.

4. CONLUCSION

In summary, we have numerically demonstrated the forward and backward propagation of SPs on thin metallic films, which is related to the positive and negative group velocity of SPs, respectively. The physical origin of the negative group velocity for backward SPs is given. Furthermore, the negative refraction of SPs is proposed by incorporating two plasmon modes with opposite group velocities. Since more energy is concentrated inside the metal for the SPs with negative group velocities, the loss will be a serious problem. Potential experiments to demonstrate negative refraction of surface waves may work on the phonon polaritons of SiC in the infrared region (these modes are low loss). Also, forward and backward propagation characteristics of magnetic surface plasmons have been theoretically reported[19], which is worth further experimental exploration.

5. ACKNOLEGEMENT

This work was supported by NSF on Nanoscale Science and Engineering Center (NSEC) (Grant No. DMI-0327077), and U.S. Air Force Office of Scientific Research MURI program under (Grant No. FA9550-04-1-0434).

6. REFERENCES

1. V. G. Veselago, "The electrodynamics of substances with simultaneously negative values of ε and μ", *Sov. Phys. Usp*. 10(4), 509-514 (1968).
2. R. A. Shelby, D. R. Smith and S. Schultz, "Experimental verification of a negative index of refraction", *Science* 292 (5514), 77-79 (2001).
3. C. Y. Luo, M. Ibanescu, S. G. Johnson and J. D. Joannopoulos, "Cerenkov radiation in photonic crystals", *Science* 299(5605), 368-371 (2003).
4. J. B. Pendry, "Negative refraction makes a perfect lens", *Phys. Rev. Lett.* 85(18), 3966-3969 (2000).
5. D. R. Smith, J. B. Pendry and M. C. K. Wiltshire, "Metamaterials and negative refractive index", *Science* 305(5685), 788-792 (2003).
6. E. Cubukcu, K. Avdin, E. Ozbay, S. Foteinopoulos and C. M. Soukoulis, "Negative refraction by photonic crystals", *Nature* 423(6940), 604-605 (2003).
7. D. R. Smith and N. Kroll, "Negative refractive index in left-handed materials", *Phys. Rev. Lett.* 85(14), 2933-2936 (2000).
8. S. Foteinopoulou and C. M. Soukoulis, "Negative refraction and left-handed behavior in two-dimensional photonic crystals", *Phys. Rev. B.* 67(23), 235107 (2003).
9. H. Raether, "Surface Plasmons", Springer, Berlin (1988).
10. W. L. Barnes, A. Dereux and T. W. Ebbesen, "Surface plasmon subwavelength optics", *Nature* 424(6950), 824-830 (2003).
11. E Ozbay, "Plasonics; merging photonics and electronics at nanoscale dimensions", *Science* 311(5758), 189-193 (2006).
12. N. Fang, H. Lee, C. Sun and X. Zhang, "Sub-diffraction-limited optical imaging with a silver superlens", *Science* 308(5721), 534-537 (2005).
13. E. N. Economou, "Surface plasmons in thin films", Phys. Rev. 182(2), 539-554 (1969).
14. M. Fukui, V. C. Y. So and R. Normandin, "Lifetimes of surface-plasmons in thin silver films", *Phys. Sta. Sol. B* 91(1), 61-64 (1979).
15. D. Sarid, "Long-range surface-plasma waves on very thin metal films", *Phys. Rev. Lett.* 37(26), 1927-1930 (1981).

16. P. B. Johnson and R. W. Christy, “Optical constants of the noble metals”, *Phys. Rev. B* 6(12), 4370-4379 (1972).
17. P. Tournois and V. Laude, “Negative group velocities in metal-film optical waveguides”, *Opt. Com.* 137(1-3), 41-45 (1997).
18. H. Shin and S. H. Fan, “All-angle negative refraction for surface plasmon waves using a metal-dielectric-metal structure”, *Phys. Rev. Lett.* 96(7), 073907 (2006).
19. J. W. Yoon, S. H. Song, C. H. Oh and P. S. Kim, “Backpropagating modes of surface polaritons on a cross-negative interface”, *Opt. Exp.* 13(2), 417-427 (2005).